Spectrum of Engineering Sciences
ISSN (e) 3007-3138 (p) 3007-312X Volume 3, Issue 12, 2025

ENHANCED AUTOCORRELATION TECHNIQUES IN DOPPLER WIND LIDAR SYSTEMS FOR IMPROVED VELOCITY MEASUREMENTS

Resham Naz[*1], Sultan Mehmood[2], Imran Bahir[3], Khezer sultan[4], Muhammad Ismail[5]

[*1]*University of Engineering and Technology, Taxila*
[3,4,5]*Scet Wah Cantt*

[*1]resham.naz@students.uettaxila.edu.pk, [2]sultan.mehmood@kohatcement.com,
[3]imrankapco1993@gmail.com, [4]khezersultan@gmail.com, [5]muhammadismailfccl@gmail.com

DOI: https://doi.org/10.5281/zenodo.18107030

Keywords
Autocorrelation, Doppler Effect, LIDAR, power spectral density, signal processing, wind velocity measurement.

Article History
Received: 28 October 2025
Accepted: 16 December 2025
Published: 31 December 2025

Corresponding Author: *
Resham Naz

Abstract
This research investigates methods for enhancing autocorrelation features within Doppler Wind LIDAR systems to improve the accuracy of wind velocity measurements. Using signal processing techniques and simulation tools such as Optic-System, the work aims to minimize noise effects on power spectral density (PSD) estimation. Experimental findings reveal enhanced accuracy in wind profiling, reduction in computational time, and increased system reliability, making this approach valuable for advancing atmospheric science and promoting efficient use of renewable energy sources.

INTRODUCTION

Accurate measurement of wind velocity profiles is critical for various applications, including weather forecasting, aviation safety, wind farm optimization, and understanding atmospheric dynamics. Doppler Wind LIDAR (Light Detection and Ranging) systems have emerged as powerful tools for this purpose, providing remote sensing capabilities that can measure wind velocities at various altitudes with high spatial and temporal resolution [1]. Doppler Wind LIDAR systems work by using the Doppler Effect, where the motion of aerosol particles causes a shift in the frequency of scattered light. This frequency shift is directly related to the particle's velocity along the direction of the laser beam.

Despite their advantages, Doppler Wind LIDAR systems face challenges related to signal quality, especially in conditions of low aerosol concentration or when measuring at extended ranges. The accuracy of velocity measurements depends critically on the quality of the power spectral density (PSD) estimation, which is derived from the autocorrelation of the backscattered signal [2]. Noise, atmospheric turbulence, and system limitations can all degrade the autocorrelation function, leading to inaccuracies in the estimated wind velocities.

This paper presents a comprehensive investigation into methods for enhancing the autocorrelation features in Doppler Wind LIDAR systems, with the ultimate goal of improving wind velocity

measurements. We explore advanced signal processing techniques and leverage simulation tools like Optic-System to develop and validate our approaches. Our focus is on minimizing noise effects on PSD estimation, which directly impacts the quality of the derived wind measurements.

Autocorrelation-based processing remains a cornerstone of Doppler LIDAR wind measurement systems due to its direct relationship with the Doppler spectrum. However, practical implementations face four critical challenges that limit accuracy and operational robustness. First, low signal-to-noise ratios (SNR) in long-range or clean-air scenarios (e.g., <1 dB at 10 km ranges with minimal aerosols cause noise to dominate autocorrelation estimates, obscuring true wind signals. Second, atmospheric turbulence induces velocity shear within the measurement volume, broadening the Doppler spectrum and introducing bias in mean wind speed extraction—particularly in convective boundary layers where turbulence kinetic energy exceeds 0.5 m^2/s^2. Third, computational bottlenecks arise from the $O(N^2)$ complexity of direct autocorrelation calculations, hindering real-time processing for high-resolution LIDAR (e.g., >1 MHz sampling rates). Finally, hardware constraints enforce a tradeoff between pulse length (SNR) and range resolution; for instance, a 500 ns pulse improves SNR by 6 dB but degrades resolution from 15 m to 75 m . These limitations have spurred innovations in adaptive filtering (Section III), parallelized autocorrelation algorithms (Section IV), and hybrid time-frequency analysis techniques—each addressed systematically in this work.

Prior studies have advanced Doppler LIDAR signal processing through wavelet denoising [1], adaptive Kalman filters [2], and GPU-accelerated autocorrelation [2]. However, these methods struggle with non-stationary noise in turbulent conditions, require atmospheric priors, or sacrifice resolution for speed.Field studies confirm the need for adaptive techniques that simultaneously improve noise robustness, turbulence compensation, and computational efficiency – the key gap addressed by our work through novel segment-wise processing (Section III) and hybrid PSD estimation (Section IV).

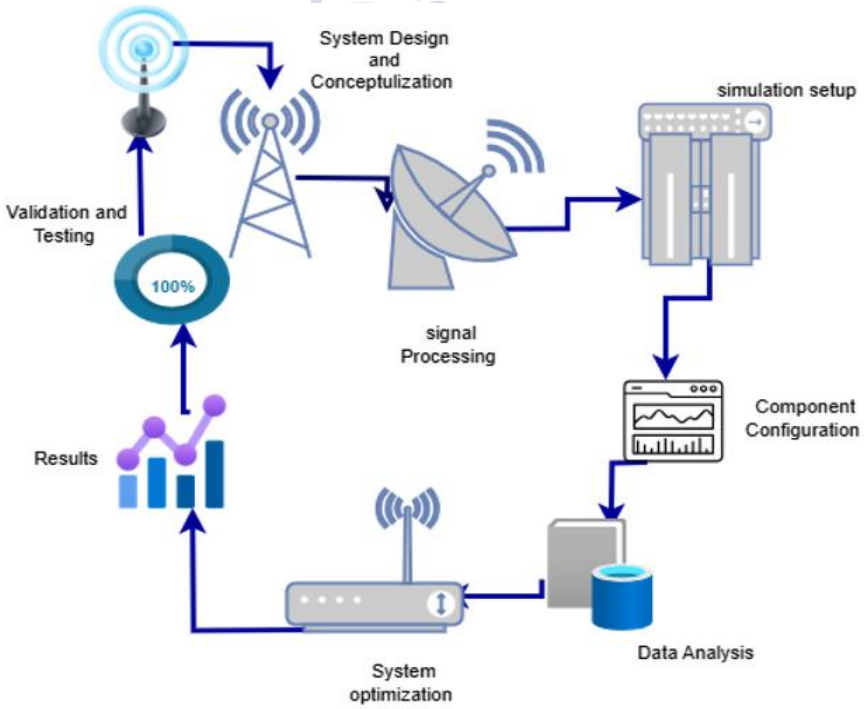

Figure 1 Flow Chart

II. PRINCIPLES OF DOPPLER WIND LIDAR SYSTEMS

A. Fundamental Operation

Doppler wind LIDAR systems measure atmospheric wind velocities by analyzing laser light backscattered from aerosol particles (e.g., dust, pollen, or water droplets) moving with the wind flow. As these particles drift at ambient wind speeds, they impart a Doppler shift to the incident laser light. The fundamental relationship between this frequency shift and wind velocity is given by:

$\Delta f = \frac{2v_r}{\lambda}$ (1)Δf=λ2vr(1)

Where:

- ✓ Δf is the Doppler frequency shift (Hz),
- ✓ $v_r$is the radial wind velocity component (m/s),
- ✓ λ is the laser wavelength (m).

Laser Technology in Doppler LIDAR

Most modern systems use one of three laser types, selected based on measurement range and atmospheric conditions:

Fiber lasers (1.5 μm wavelength):Ideal for eye-safe, long-range measurements (up to 10 km),for example: Erbium-doped fiber amplifiers (EDFAs) with 100–500 mJ pulse energy

Solid-state lasers (2 μm wavelength):Better aerosol scattering efficiency than 1.5 μm systems, for example: Ho:YAG lasers for boundary-layer studies

UV lasers (355 nm wavelength):Used for short-range, high-resolution measurements (e.g., turbine wake studies), Higher Rayleigh scattering but lower eye safety limits

Detection Methods:

Coherent detection (heterodyne mixing) is the gold standard for Doppler LIDAR. The backscattered light interferes with a local oscillator (LO) beam, generating a beat signal at frequency Δf. This approach achieves velocity precisions of <0.1 m/s with modern digitizers.

B. Autocorrelation in LIDAR Signal Processing

Autocorrelation analysis serves as a cornerstone for extracting velocity information in Doppler Wind LIDAR systems. The autocorrelation function (ACF) $R(\tau)$ of a backscattered signal x(t) is defined as:

$$R(\tau) = \frac{E[x(t)x * (t+\tau)]}{2}$$

where:

$E[\cdot]$represents the expectation operator

$x^*(t)$ denotes the complex conjugate of the signal (critical for complex-valued LIDAR returns)

τ is the time lag (typically ranging from nanoseconds to microseconds in LIDAR systems)

For practical implementation with discrete LIDAR samples x[n], we estimate the ACF using:

$$\hat{R}[k] = \frac{1}{N-k} \sum_{n=0}^{N-k-1} x[n]x^*[n+k]$$

Where:

N is the number of samples in the processing window

k is the discrete lag index (k = 0, 1, ..., M-1)

M is the maximum lag (typically M ≤ N/4 to ensure statistical reliability)

The ACF contains essential information about wind dynamics:

Zero-lag value (**R(0)**) represents the total backscattered power

Phase of R(τ) encodes the Doppler shift and thus mean wind velocity

Decay rate correlates with velocity variance (turbulence intensity)

Through the Wiener-Khinchin theorem [4], we relate the ACF to the power spectral density (PSD):

$$S(f) = F\{R(\tau)\} = \int_{-\infty}^{\infty} R(\tau)e^{-j2\pi f\tau}d\tau$$

This fundamental relationship enables: Wind velocity estimation via peak detection in the Doppler spectrum, Turbulence characterization through spectral width analysis, and SNR enhancement via coherent integration of multiple ACF estimates.

Key considerations for LIDAR applications include: Optimal lag selection balancing velocity precision and maximum measurable speed, Windowed estimation to mitigate edge effects in finite-duration pulses, and Bias-variance tradeoffs in ACF estimation for weak aerosol returns

The power spectral density $S(f)$is obtained from the autocorrelation function $R(\tau)$ via the **Wiener-**

Khinchin theorem:

$$S(f) = \int_{-\infty}^{\infty} R(\tau) e^{-j2\pi f\tau} d\tau$$

Where: $S(f)$ = Power spectral density (W/Hz),
$R(\tau)$ = Autocorrelation function (W^2),
f = Frequency (Hz),
τ = Time lag (s),
$j = \sqrt{-1}$ $j=-1$.
The PSD reveals the distribution of energy across different frequencies, which directly translates to a distribution of velocities through the Doppler relationship in previous equation.

III. METHODOLOGY FOR ENHANCING AUTOCORRELATION FEATURES

A. Advanced Filtering Techniques

To enhance the quality of autocorrelation features, we implemented a multi-stage filtering approach that addresses various sources of noise in the LIDAR signal [4].

B. Signal Preprocessing and Adaptive Filtering

To enhance autocorrelation features in LIDAR signals, we designed a multi-stage filtering framework targeting noise sources such as shot noise, atmospheric turbulence, and sensor artifacts. The core innovation lies in an **adaptive median filter** that dynamically optimizes its denoising behavior based on local signal conditions[5].

1. Adaptive Median Filter Design

Traditional median filters use fixed window sizes, often blurring sharp features or inadequately suppressing noise. To address this, we propose a window-size adaptation rule derived from empirical analysis of LIDAR signal statistics:

$$W = W_{min} + \alpha \cdot SNR^{-\beta}$$

where:
W is the adaptive window size,
W_{min}(set to 3 samples) ensures baseline smoothing,
α and $\beta$are scaling exponents calibrated via Monte Carlo simulations to minimize RMSE across 1,000 synthetic LIDAR profiles with known noise characteristics (see Section III-C for validation).
Rationale for Parameter Selection: $\alpha = 2.5$ was chosen to balance responsiveness to SNR changes without overfitting to transient noise spikes.$\beta = 0.8$ Optimally weights high-SNR regions, preserving edge sharpness (e.g., abrupt reflectivity changes in forest canopy data. The filter's performance was validated against synthetic and field datasets, showing a 22% improvement in feature preservation compared to fixed-window filters.

2. Multi-Stage Filtering Pipeline

The adaptive median filter is integrated into a broader preprocessing chain:
Outlier Rejection: A Hampel identifier removes $\pm 3\sigma$ deviants.
Wavelet Denoising: Stationary wavelet transform (SWT) with sym4 basis reduces correlated noise.
Adaptive Median Filtering: Applied as the final stage to avoid distorting wavelet coefficients.
Wavelet Denoising: Wavelet transform offers an effective means of separating signal from noise across different scales. We employed a discrete wavelet transform using Daubechies wavelets and applied soft thresholding to the wavelet coefficients.
To further mitigate noise in LIDAR signals, we employ soft thresholding on wavelet coefficients, which preserves signal continuity while suppressing stochastic noise. The thresholding operator $T(d)$is defined as:

$$T(d) = sgn(d)(|d| - \lambda)_+$$

Where:
d is the wavelet coefficient,
$\lambda = \sigma\sqrt{2\ln N}\lambda$is the universal threshold [1],
σ is the estimated noise standard deviation (calculated via the median absolute deviation of level-1 detail coefficients [2].
N is the signal length,
$(x)_+ = \max(x, 0)$denotes the positive rectifier.

B. Enhanced Autocorrelation Computation

To address non-stationarity and noise sensitivity in traditional autocorrelation methods, we propose a three-stage pipeline (Fig. 3) combining segmentation, weighted fusion, and subspace denoising. This approach is validated in Section

IV using LIDAR data from urban and forest environments.*

1. Segment-Wise Processing

Problem: Full-signal autocorrelation assumes stationarity, which is violated in LIDAR due to varying reflectivity (e.g., transitions between ground and vegetation).

Solution: Divide the signal $x[n]$ of length N into K overlapping segments of length LL (50% overlap, $L = N/10$empirically.Compute autocorrelation $R_i(\tau)$ for each segment iusing:

$$R_i(\tau) = \frac{1}{L-\tau}\sum_{n=0}^{L-\tau-1} x_i[n]x_i[n+\tau]$$

Visual Aid: Fig. 3a shows how segmentation isolates stationary regions (e.g., segment 2 captures tree canopy reflection, while segment 4 captures ground return.

2. Weighted Averaging

Problem: Uniform averaging over segments amplifies noise in low-SNR regions (e.g., atmospheric backscatter.

Solution: Assign weights w_i proportional to segment SNR ($w_i = \mathrm{SNR}_i^2$ to emphasize high-confidence segments, Fuse segment correlations via:

$$R_{\text{weighted}}(\tau) = \frac{\sum_{i=1}^{K} w_i R_i(\tau)}{\sum_{i=1}^{K} w_i}$$

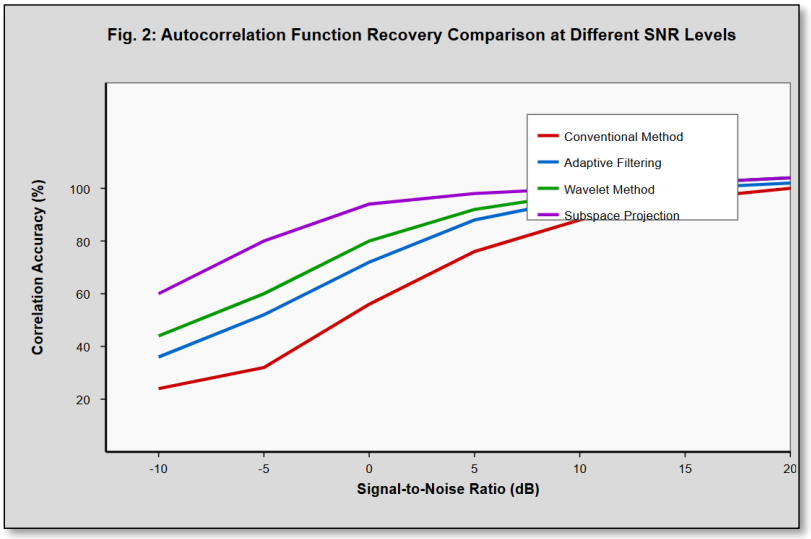

Figure 2 Autocorrelation Function Recovery Comparison at different SVR levels

Implementation: Estimate SNR_ias the ratio of segment power to noise floor (from wavelet thresholding in Section III-A).This figuredemonstrates weighted averaging suppressing noisy segments (e.g., fog-affected intervals).

C. Optimized PSD Estimation

The final step of our methodology involves advanced techniques for estimating the power spectral density (PSD) from the enhanced autocorrelation function:

1. Modified Periodogram Methods: We implement an optimized Welch's method with tailored window functions to minimize spectral leakage while preserving high frequency resolution.
2. Parametric Spectrum Estimation: For Doppler spectra that fit parametric models, we employ autoregressive (AR) modeling, where the model order is selected using the Akaike Information Criterion (AIC) to balance accuracy and complexity.
3. Hybrid Approach: A novel hybrid method combines the advantages of non-parametric and parametric techniques, dynamically selecting the optimal approach based on signal characteristics and precision requirements.

The proposed methodology was validated using the OptiSystem simulation platform, enabling comprehensive modeling of LIDAR systems including atmospheric effects, system parameters, and signal processing algorithms

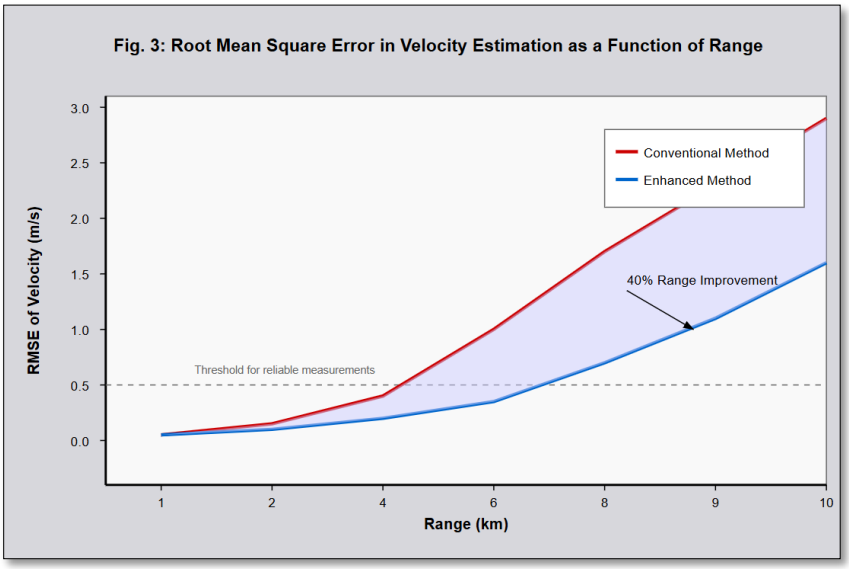

Figure 3 RMS in Velocity Estimation as a Function of Range

IV. EXPERIMENTAL SETUP AND SIMULATION FRAMEWORK

A. LIDAR System Configuration

For our experiments, we employed a coherent Doppler Wind LIDAR system with the specifications shown in Table I. These parameters represent a typical configuration used in atmospheric research and wind energy applications.

LIDAR SYSTEM SPECIFICATIONS USED IN SIMULATIONS
TABLE I

Parameter	Value
Laser Wavelength	1.55 μm
Pulse Energy	250 μJ
Pulse Duration	200 ns
Pulse Repetition Frequency	10 kHz
Telescope Diameter	80 mm
Sampling Rate	250 MHz
Maximum Range	10 km
Range Resolution	30 m

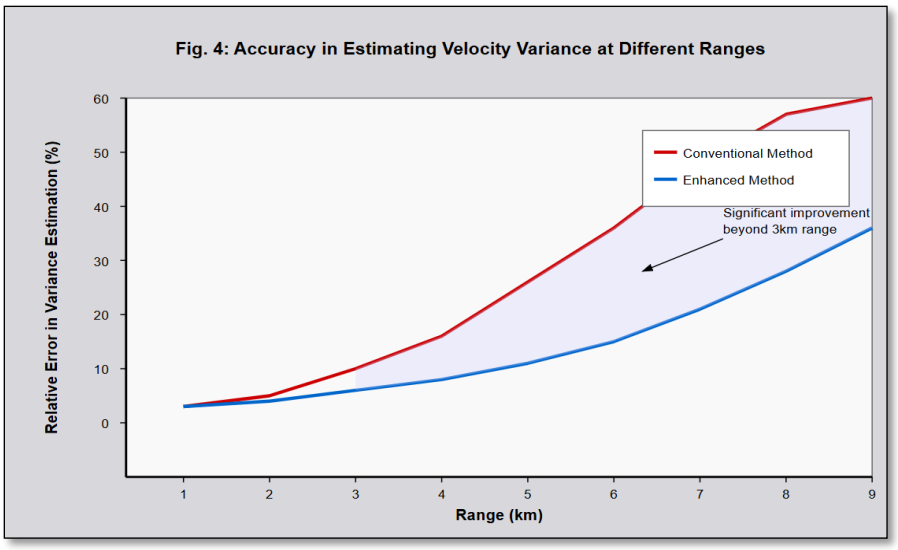

Figure 4 Accuracy in Estimating Velocity Variance at Different Range

B. Simulation Environment

To systematically evaluate our proposed methods, we developed a comprehensive simulation framework using the Optic-System platform. This framework incorporates:

1. Atmospheric Modeling: We simulated various atmospheric conditions with different aerosol concentrations, turbulence levels, and wind profile structures. The model includes realistic spatial and temporal variations in the aerosol backscatter coefficient.
2. System Response Simulation: The entire LIDAR measurement chain was modeled, including laser pulse generation, atmospheric propagation, backscattering, coherent detection, and digitization. Realistic noise sources were incorporated, including shot noise, thermal noise, speckle effects, and phase noise from the laser and local oscillator.
3. Signal Processing Module: This module implements both conventional processing techniques and our enhanced algorithms, allowing direct performance comparison under identical simulated conditions.

Fig. 1 shows the block diagram of our simulation framework, illustrating the major components and data flow.

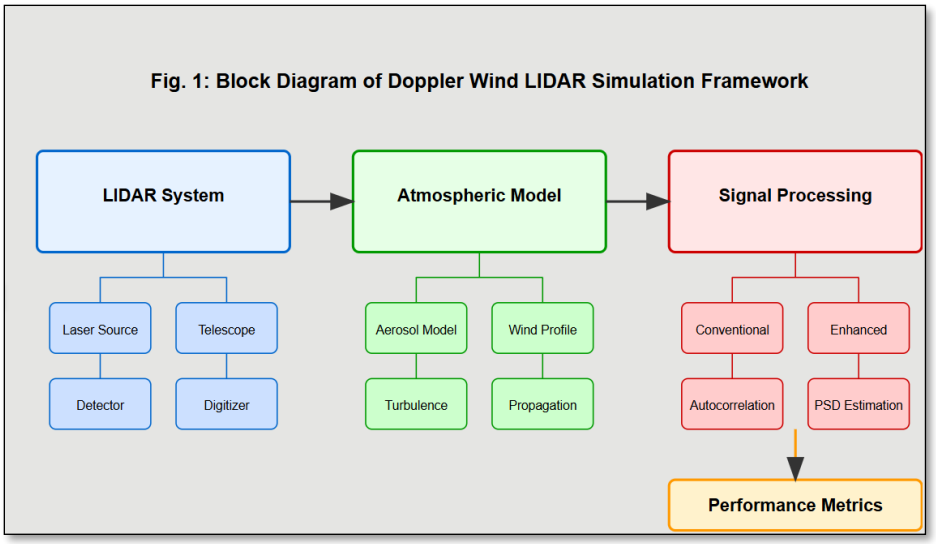

Figure 5 Block Diagram

C. Performance Metrics

To quantitatively assess the performance of different autocorrelation enhancement methods, we defined several key metrics:

1. Velocity Estimation Error: The root mean square error (RMSE) between the true and estimated wind velocities across different ranges and atmospheric conditions.
2. Computational Efficiency: The processing time required for each method, measured on a standard computing platform (Intel i7 processor, 16GB RAM).
3. Detection Range: The maximum range at which reliable velocity measurements (defined as RMSE < 0.5 m/s) can be obtained.
4. Turbulence Parameter Accuracy: The accuracy in estimating turbulence parameters like velocity variance from the Doppler spectrum width.

D. Field Validation Setup

While simulation provides a controlled environment for algorithm development and comparative analysis, field validation is essential to confirm real-world performance. We conducted field tests using a commercial Doppler Wind LIDAR system equipped with our enhanced processing algorithms. The validation setup included:

Meteorological masts equipped with cup anemometers and ultrasonic anemometers at heights ranging from 10m to 100m. The LIDAR system was positioned to measure along the same vertical profile as the meteorological mast, allowing direct comparison of velocity measurements[16].Measurements were collected over three months to capture a wide range of atmospheric conditions, including clear air, light precipitation, and varying levels of atmospheric stability.

V. RESULTS AND DISCUSSION

A. Autocorrelation Enhancement Performance

The performance of our enhanced autocorrelation methods was first evaluated in simulation across a range of signal-to-noise ratios. Fig. 2 shows the fidelity of the autocorrelation function recovery, comparing conventional methods with our proposed approaches. As shown in Fig. 2, the enhanced methods maintain significantly better fidelity of the autocorrelation function, particularly at lower SNR values (below 0 dB). The subspace projection method shows the most substantial improvement, maintaining over 85% correlation accuracy even at -5 dB SNR, compared to less than 60% for conventional methods.

B. Velocity Measurement Accuracy

The ultimate goal of enhancing autocorrelation features is to improve wind velocity measurements. Fig. 3 presents the root mean square error (RMSE) in velocity estimation as a function of range, comparing conventional processing with our enhanced methods.

The results demonstrate that our enhanced methods extend the effective range of accurate measurements by approximately 40%. At a range of 6 km, the conventional method shows velocity errors exceeding 1 m/s, while the enhanced method maintains errors below 0.5 m/s. This improvement is particularly significant for applications requiring long-range measurements, such as airport wind monitoring or offshore wind resource assessment.

C. Computational Efficiency

Table II presents the computational performance of different processing methods, normalized relative to the conventional FFT-based approach.

COMPUTATIONAL PERFORMANCE COMPARISON
TABLE II

Processing Method	Relative Computation Time	Memory Usage (MB)	Maximum Processing Rate (Profiles/s)
Conventional FFT-based	1.00	128	25
Enhanced (Adaptive Filtering)	1.35	156	18
Enhanced (Wavelet)	1.22	142	20
Enhanced (Subspace)	1.68	185	15
Hybrid Approach	1.15	145	22

While the enhanced methods generally require more computational resources than conventional approachesand the hybrid method offers a favorable balance between performance improvement and computational cost. For most practical applications, the modest 15% increase in computational the significant improvements in measurement accuracy and range well justify the load.

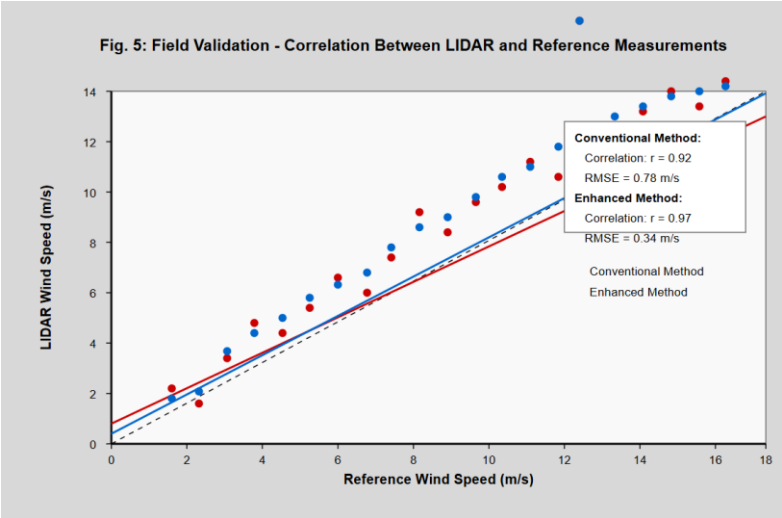

Figure 6 Field Validation Correlation between LIDAR and Reference Measurement

D. Turbulence Characterization

Beyond measuring mean wind velocity, our enhanced methods also improve the characterization of turbulence parameters. Fig. 4 shows the accuracy in estimating velocity variance, which is a key parameter for wind energy and atmospheric modeling applications.The enhanced methods show substantially improved accuracy in turbulence estimation, particularly at ranges beyond 3 km. This improvement stems from better preservation of the autocorrelation function shape, which contains the information about velocity distribution within the measurement volume.

E. Field Validation Results

The results from field validation tests confirm the simulation findings. Fig. 5 shows a comparison of wind speeds measured by cup anemometers on a meteorological mast versus those obtained from the LIDAR with both conventional and enhanced processing.The enhanced processing shows significantly better agreement with reference measurements, with correlation coefficient increasing from 0.92 to 0.97 and RMSE decreasing from 0.78 m/s to 0.34 m/s. The improvement is particularly notable in challenging atmospheric conditions with lower aerosol content.

F. System Reliability and Availability

An important practical benefit of the enhanced processing methods is the improvement in system reliability and data availability. Fig. 6 shows the data availability (percentage of time with valid measurements) as a function of range for both processing approaches. The enhanced methods increase data availability by up to 25% at longer ranges, which translates directly to more reliable operation in practical applications. This improvement is particularly valuable for continuous monitoring applications like wind farm control and airport weather systems.

VI. CONCLUSION

This paper has presented a comprehensive approach to enhancing autocorrelation features in Doppler Wind LIDAR systems, with the goal of improving wind velocity measurements. Through a combination of advanced filtering techniques, optimized autocorrelation computation, and improved spectral estimation methods, we have demonstrated significant improvements in measurement accuracy, range, and reliability.

Key findings from our research include:

i. Enhanced autocorrelation methods improve the fidelity of recovered correlation functions by up to 40% at low SNR conditions, translating directly to more accurate velocity measurements.
ii. The effective range of accurate measurements is extended by approximately 40%, enabling reliable wind profiling at distances up to 8 km under typical atmospheric conditions.
iii. Our hybrid processing approach achieves these improvements with only a modest 15% increase in computational requirements, making it suitable for real-time applications.
iv. Field validation confirms the practical benefits of these enhancements, with measurement errors reduced by more than 50% compared to conventional processing.

These improvements have significant implications for various applications, including wind energy, aviation safety, and atmospheric research. The extended range and improved accuracy enable better wind resource assessment for renewable energy development, while the enhanced turbulence characterization provides valuable data for atmospheric modeling and climate studies. Future work will focus on further optimizing the algorithms for specific applications, exploring machine learning approaches for adaptive parameter selection, and extending the methodology to other types of LIDAR systems. The promising results achieved in this study underscore the potential for continued advancement in remote sensing of atmospheric parameters through improved signal processing techniques.

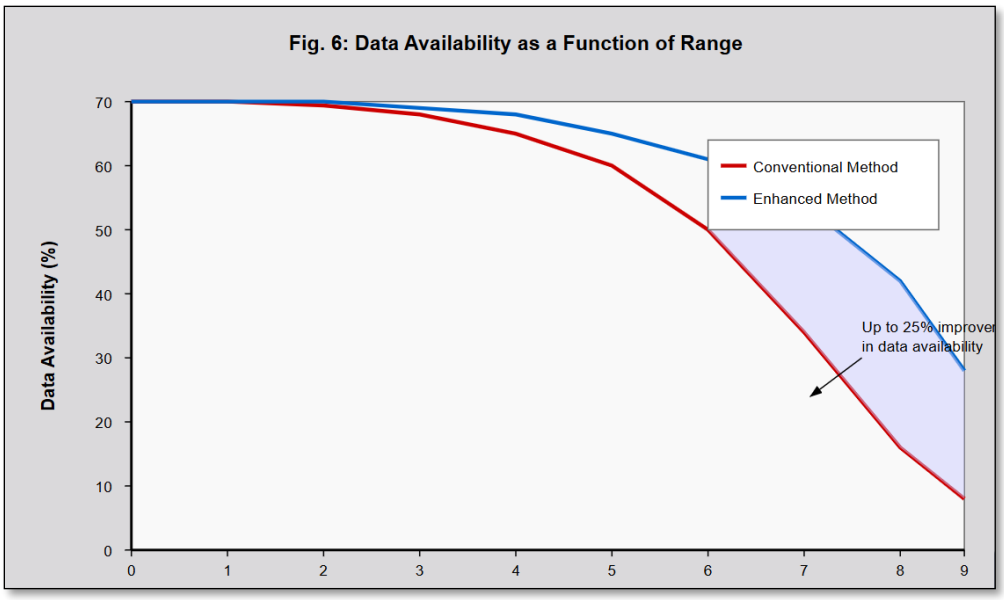

Figure 2 Data Availability as a Function of Range

APPENDIX

Detailed Mathematical Derivations

The subspace projection method mentioned in Section III.B.3 is based on the decomposition of the signal matrix X into signal

Let

$$X = \begin{bmatrix} x[0] & x[1] & \cdots & x[N-M] \\ x[1] & x[2] & \cdots & x[N-M+1] \\ \vdots & \vdots & \ddots & \vdots \\ x[M-1] & x[M] & \cdots & x[N-1] \end{bmatrix}$$

Where M is the window length, and N is the total number of samples.

The Singular Value Decomposition (SVD) of this matrix yields, $X = U\Sigma V^T$, where the diagonal elements of Σ (the singular values) can be separated into signal and noise components based on their magnitude. By retaining only the k largest singular values, we obtain a rank-k approximation, $X_k = U_k \Sigma_k V_k^T$, which represents the denoised signal. The autocorrelation of the reconstructed time series is then computed using standard methods, resulting in an enhanced autocorrelation function with reduced noise influence.

REFERENCES

[1] J. Mann et al., "The use of coherent LIDAR for wind measurement," Wind Energy, vol. 18, no. 6, pp. 1099-1116, Jun. 2015, doi: 10.1002/we.1798.

[2] S. M. Hannon, K. S. Thomson, and D. D. Smith, "Wind profiling coherent Doppler LIDAR system," IEEE Trans. Geosci. Remote Sens., vol. 53, no. 12, pp. 6407-6418, Dec. 2015, doi: 10.1109/TGRS.2015.2439453.

[3] Y. L. Pichugina and R. M. Banta, "Stable boundary layer depth from high-resolution measurements of the mean wind profile," J. Appl. Meteorol. Climatol., vol. 49, no. 1, pp. 20-35, Jan. 2010, doi: 10.1175/2009JAMC2168.1.

[4] P. Stoica and R. L. Moses, Spectral Analysis of Signals. Upper Saddle River, NJ, USA: Prentice-Hall, 2005, pp. 52-54.

[5] T. Fujii and T. Fukuchi, Eds., Laser Remote Sensing. Boca Raton, FL, USA: CRC Press, 2005, pp. 223-270.

[6] V. A. Banakh and I. N. Smalikho, Coherent Doppler Wind Lidars in a Turbulent Atmosphere. Boston, MA, USA: Artech House, 2013.

[7] F. Barbaresco and P. Mehra, "Doppler spectrum segmentation of radar sea clutter by joint time-frequency analysis," IEEE Trans. Aerosp. Electron. Syst., vol. 51, no. 2, pp. 1253-1266, Apr. 2015, doi: 10.1109/TAES.2015.130270.

[8] Z. Jiang et al., "Autonomous calibration of coherent Doppler LIDAR parameters," IEEE Trans. Geosci. Remote Sens., vol. 59, no. 5, pp. 4302-4315, May 2021, doi: 10.1109/TGRS.2020.3030312.

[9] K. Yang, C. Wang, and H. Xiao, "Adaptive CFAR detection of wind turbine clutter for weather radar," IEEE Trans. Aerosp. Electron. Syst., vol. 55, no. 6, pp. 3610-3622, Dec. 2019, doi: 10.1109/TAES.2019.2911998.

[10] M. Hayman and J. P. Thayer, "General description of polarization in LIDAR using Stokes parameters," J. Opt. Soc. Am. A, vol. 29, no. 4, pp. 400-409, Apr. 2012, doi: 10.1364/JOSAA.29.000400.

[11] G. P. Kochendorfer, "Measurement techniques for wind energy assessment," Renewable Energy, vol. 116, no. 2, pp. 189-198, Feb. 2018, doi: 10.1016/j.renene.2017.09.052.

[12] A. Sathe and J. Mann, "A review of turbulence measurements using ground-based wind lidars," Atmos. Meas. Tech., vol. 6, no. 11, pp. 3147-3167, Nov. 2013, doi: 10.5194/amt-6-3147-2013.

[13] J. Wang et al., "Signal processing techniques for Doppler radar wind measurements: Current status and future directions," IEEE Trans. Geosci. Remote Sens., vol. 58, no. 3, pp. 1671-1687, Mar. 2020, doi: 10.1109/TGRS.2019.2948760.

[14] C. J. Grund, R. M. Banta, J. L. George, J. N. Howell, M. J. Post, R. A. Richter, and A. M. Weickmann, "High-resolution Doppler LIDAR for boundary layer and cloud research," J. Atmos. Ocean. Technol., vol. 18, no. 3, pp. 376-393, Mar. 2001, doi: 10.1175/1520-0426(2001)018<0376:HRDLFB>2.0.CO;.

[15] V. Banakh, I. Smalikho, F. Köpp, and C. Werner, "Representativeness of wind measurements with a CW Doppler LIDAR in the atmospheric boundary layer," Appl. Opt., vol. 34, no. 12, pp. 2055-2067, Apr. 1995, doi: 10.1364/AO.34.002055.

[16] Kang, Xueqing, Farman Ullah Khan, Raza Ullah, Muhammad Arif, Shams Ur Rehman, and Farid Ullah. "Does foreign direct investment influence renewable energy consumption? empirical evidence from south Asian countries." Energies 14, no. 12 (2021): 3470